Dalton Transactions

Accepted Manuscript

ROYAL SOCIETY OF CHEMISTRY

www.rsc.org/dalton

Cite this: DOI: 10.1039/c0xx00000x

www.rsc.org/xxxxxx

ARTICLE TYPE

Predominance of Covalency in Water-Vapor-Responsive MMX-Type Chain Complexes Revealed by ^{129}I Mössbauer Spectroscopy

Hiroaki Iguchi,*[a,b] Shinji Kitao,[c] Makoto Seto,[c] Shinya Takaishi[a,b] and Masahiro Yamashita*[a,b]

Received (in XXX, XXX) Xth XXXXXXXXX 20XX, Accepted Xth XXXXXXXXX 20XX

DOI: 10.1039/b000000x

^{129}I Mössbauer spectroscopy was applied to water-vapor-responsive MMX-type quasi-one-dimensional iodide-bridged Pt complexes (MMX chains) in order to investigate their electronic state quantitatively. Two sets of octuplets observed in $K_2(H_3NC_3H_6NH_3)[Pt_2(pop)_4I]\cdot 4H_2O$ (**2·4H$_2$O**) and one octuplet observed in $K_2(cis\text{-}H_3NCH_2CH{=}CHCH_2NH_3)[Pt_2(pop)_4I]\cdot 4H_2O$ (**1·4H$_2$O**) and dehydrated complexes (**1** and **2**) indicate a unique alternating charge-polarization + charge-density-wave (ACP+CDW) electronic state and charge-density-wave (CDW) electronic state, respectively. These spectra correspond to their crystal structure and the change of electronic states upon dehydration. Since these complexes consist of alternating array of positively-charged and negatively-charged layers, the charge on the iodide ion (ρ_{IS}) was discussed on the basis of the isomer shift (IS). The ρ_{IS} of the water-vapor-responsive MMX chains was mainly –0.13 to –0.21, which are the smallest of all MMX chains reported so far. Hence, it indicates the negative charge on the iodide ion is strongly donated to the Pt ion in these complexes. This covalent interaction predominates in the ACP+CDW state as well as in the CDW state. Therefore, the ACP+CDW state is in fact the CDW state with the ACP-type lattice distortion. Because the ρ_{IS} became smaller with decreasing Pt–I–Pt distance, it can be concluded that the covalent interaction plays an important role in determining the electronic states of the MMX chains with pop (= $P_2H_2O_5^{2-}$) ligands.

Introduction

The electronic states in one-dimensional (1D) electron system play a key role in bringing about a variety of attractive physical properties such as high conductivity,[1,2] large optical nonlinearity,[3,4] Luttinger liquid behavior,[5] ultra-fast optical responses,[6] etc. Quasi-1D halogen-bridged metal complexes, which also show attractive physical properties originating from the 1D electron system,[4,6–8] have robust chain structure derived from the coordination bonds between the metal ions (M) and the bridging halide ions (X). Some of them show the reversible adsorption and desorption of molecules with retention of crystallinity[9–11] and with the change of the electronic states,[11] indicating that they are promising to be multifunctional vapor-induced switching materials.

Quasi-1D halogen-bridged metal complexes consisting of paddle-wheel-type dinuclear complexes, so-called MMX chains, have higher degrees of freedom of the electrons than those consisting of mononuclear complexes (MX chains), inducing larger variety of electronic states in MMX chains. On the basis of theoretical calculations[12] and experimental data, the electronic states of the MMX chains have been classified into the following four states:

(a) average-valence (AV) state

$$\text{–}M^{2.5+}\text{–}M^{2.5+}\text{—}X\text{—}M^{2.5+}\text{–}M^{2.5+}\text{—}X\text{–}$$

(b) charge-density-wave (CDW) state

$$\cdots M^{2+}\text{–}M^{2+}\cdots\cdots X\text{—}M^{3+}\text{–}M^{3+}\text{—}X\cdots$$

(c) charge-polarization (CP) state

$$\cdots M^{2+}\text{–}M^{3+}\text{—}X\cdots\cdots M^{2+}\text{–}M^{3+}\text{—}X\cdots$$

(d) alternating charge-polarization (ACP) state

$$\cdots M^{2+}\text{–}M^{3+}\text{—}X\text{—}M^{3+}\text{–}M^{2+}\cdots\cdots X\cdots$$

These electronic states are strongly correlated to the position of the bridging halide ion, which is at the midpoint between two metal ions in the AV state and is close to the higher-oxidized metal ion in other states. Strictly, formal oxidation numbers, 3+ and 2+, should be represented as $(3\text{-}\delta)$+ and $(2+\delta)$+, respectively. The AV state is a Robin-Day class III system, whereas the other three are class II systems.[13]

MMX chains synthesized to date are classified into two categories on the basis of their ligands. A high conductivity,[14] metal-insulator transition,[14] and the formation of nanowires on a substrate[15] have been reported in a dithioacetate (dta) system, $[M_2(RCS_2)_4I]$ (M = Ni, and Pt; R = alkyl chain group). However, the adjustable components are limited to the metal ions (Ni and Pt) and the alkyl chain groups in the dta system. On the other hand, in a diphosphite (pop) system, $Y_4[Pt_2(pop)_4X]\cdot nH_2O$ and $Y'_2[Pt_2(pop)_4X]\cdot nH_2O$ (Y = alkali metal, alkyl ammonium, etc.; Y' = alkyldiammonium; X = Cl^-, Br^-, and I^-; pop = $P_2H_2O_5^{2-}$),[11,16] the negatively charged chains require countercations, of which there are a huge number of possible candidates. Furthermore, removing lattice water molecules can change the electronic states of the MMX chains.[11] Therefore, the pop system is more promising target to realize the new electronic states and

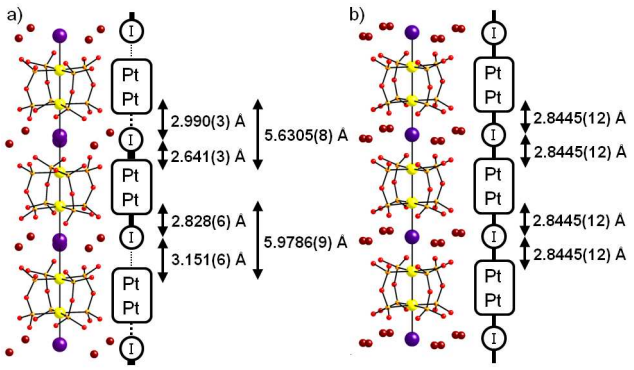

Fig. 1 Crystal structure, Pt–I and Pt–I–Pt distance of a) **2·4H$_2$O** and b) **2**. H$_2$O molecules and $H_3NC_3H_6NH_3^{2+}$ ions are omitted for clarity. Iodide ions of **2·4H$_2$O** and K^+ ions of **2** are disordered. Pt yellow, I purple, K brown, P orange, O red, N blue, C black

to study the change of electronic states upon chemical external stimuli such as adsorption-desorption of molecules.

Recently, we rationally designed more robust MMX chains with binary countercations, $A_2B[Pt_2(pop)_4I]\cdot nH_2O$ (A^+ = K^+ and Rb^+; B^{2+} = aliphatic diammonium ion; n = 2 and 4),[17] which show reversible dehydration/rehydration when B^{2+} is $H_3NCH_2CHXCH_2NH_3^{2+}$ (X = H, Me, Cl) or *cis*/*trans*-$H_3NCH_2CH{=}CHCH_2NH_3^{2+}$.[17b,c] Although the electronic state of K_2(*cis*-$H_3NCH_2CH{=}CHCH_2NH_3$)$[Pt_2(pop)_4I]\cdot 4H_2O$ (**1·4H$_2$O**) is typical CDW state,[17c] $K_2(H_3NC_3H_6NH_3)[Pt_2(pop)_4I]\cdot 4H_2O$ (**2·4H$_2$O**) forms a new ACP+CDW electronic state ($\cdots Pt^{(2+a)+}$–$Pt^{(2+b)+}\cdots I$–$Pt^{(3-c)+}$–$Pt^{(3-d)+}$–$I\cdots$; 0 < a, b, c, d < 0.5; a, c < b, d).[17b] Dehydration of **2·4H$_2$O** changes the structure as shown in Figure 1 and also changes the electronic state from the ACP+CDW state to the narrow-gapped CDW state,[17b] which contains thermally activated Pt^{3+} spins as mobile solitons.[18]

Estimating the charge on the metal or halide ion in MMX chains is quite important to understand the electronic states. ^{129}I Mössbauer spectroscopy is a powerful tool for determining the charge on the iodide ion quantitatively. So far, $[Pt_2(MeCS_2)_4I]$ and $[Pt_2(EtCS_2)_4I]$ forming the ACP state, $(H_3NC_6H_{12}NH_3)_2[Pt_2(pop)_4I]$ forming the CDW state, $(Et_2NH_2)_4[Pt_2(pop)_4I]$ forming the CP state, and their precursor Pt(III)$_2$ complexes have been studied by the ^{129}I Mössbauer spectroscopy.[14d,19] Herein, we study the characteristic of the new ACP+CDW state in **2·4H$_2$O** and its change upon dehydration by comparing the similar complex, **1·4H$_2$O**, and other MMX chains in the pop system. In addition, we discuss the origin of the charge variation in the pop system.

Experimental Section

Materials

All of the commercially available chemicals were reagent grade and used as received. The starting Pt(II)$_2$ complex, $K_4[Pt_2(pop)_4]\cdot 2H_2O$ was synthesized from K_2PtCl_4 and H_3PO_3 following the reported procedures.[20]

Synthesis of ^{129}I-enriched MMX Chains

The starting Pt(III)$_2$ complex, ^{129}I-enriched $K_4[Pt_2(pop)_4I_2]$, was synthesized at Kyoto University Reactor (KUR) by using 5 mL of $Na^{129}I$ aqueous solution containing 36 mg (0.28 mmol) of ^{129}I with 105 mg (0.74 mmol) of Na_2SO_3 and 5 mg (0.17 mmol) of formaldehyde. The impurities was removed and ^{129}I-enriched $K_4[Pt_2(pop)_4I_2]$ was synthesized with following chemical reactions. The reaction temperature was roughly controlled by a hotplate.

(Reaction I)

$$2\ Na^{129}I + x\ Na_2SO_3 + y\ HCHO + x\ Ca(NO_3)_2 \rightarrow 2\ Na^{129}I + x\ CaSO_3\downarrow + 2x\ NaNO_3 + y\ HCHO$$

(Reaction II)

$$2\ Na^{129}I + 2x\ NaNO_3 + y\ HCHO + Pb(NO_3)_2 \rightarrow Pb^{129}I_2\downarrow + (2x{+}2)\ NaNO_3 + y\ HCHO$$

(Reaction III)

$$Pb^{129}I_2 + K_2CO_3 \rightarrow 2K^{129}I + PbCO_3\downarrow$$

(Reaction IV)

$$K^{129}I + {}^{127}I_2 \rightarrow K^{129}I^{127}I_2$$

(Reaction V)

$$K^{129}I^{127}I_2 + K_4[Pt_2(pop)_4]\cdot 2H_2O \rightarrow K_4[Pt_2(pop)_4I_2]\downarrow + KI + 2H_2O$$

Reactions I–V. Heated aqueous solution (5 mL) containing $Na^{129}I$ (0.28 mmol) was added 0.17 mL of 2.53 M $Ca(NO_3)_2$ aqueous solution (102 mg, 0.43 mmol), followed by the filtration of resulting white powder. The filtrate was heated at 30–40 °C overnight to slowly concentrate the solution by half. After being cooled to room temperature, the colorless crystals ($CaSO_3$) were separated by the decantation, then the solution was added 0.11 mL of 1.25 M $Pb(NO_3)_2$ aqueous solution (46 mg, 0.14 mmol). The resultant yellow powder ($Pb^{129}I_2$) was filtered and washed three times with methanol. $Pb^{129}I_2$ was again dissolved into hot water (20 mL) and was added 0.145 mL of 1.25 M K_2CO_3 aqueous solution (25 mg, 0.18 mmol) to form white suspension. After the centrifugation and the filtration, the clear solution was heated at 60–70 °C to reduce the volume to about 5 mL, cooled to room temperature, and added $^{127}I_2$ (85.3 mg, 0.336 mmol). To the resultant homogeneous solution, $K_4[Pt_2(pop)_4]\cdot 2H_2O$ (391 mg, 0.338 mmol) was added and heated at 30–40 °C for 2 h, followed by adding methanol (approx. 50 mL) to precipitate ^{129}I-enriched $K_4[Pt_2(pop)_4I_2]$. The brown solid was washed with methanol and dried by heating. (331 mg, 0.24 mmol, 85%).

^{129}I-enriched K_2(*cis*-$H_3NCH_2CH{=}CHCH_2NH_3$)$[Pt_2(pop)_4I]\cdot 4H_2O$ (1·4H$_2$O). The synthesis of **1·4H$_2$O** was carried out by following the reported procedure for non-enriched complex.[17c] 21.5 mL of the Pt_2 complexes in water (containing 165 mg (0.14 mmol) of $K_4[Pt_2(pop)_4]\cdot 2H_2O$ and 168 mg (0.12 mmol) of $K_4[Pt_2(pop)_4I_2]$) and 21 mL of the aqueous salt solution (containing 42 mg (0.20 mmol) of *cis*-$H_3NCH_2CH{=}CHCH_2NH_3(NO_3)_2$ and 808 mg (8.00 mmol) of KNO_3) were mixed and allowed to stand for 2 days. **1·4H$_2$O** was obtained as glossy brown cubic crystals. (217 mg, 68%).

^{129}I-enriched $K_2(H_3NC_3H_6NH_3)[Pt_2(pop)_4I]\cdot 4H_2O$ (2·4H$_2$O). The synthesis of **2·4H$_2$O** was carried out by following the reported procedure for non-enriched complex.[17b] 10.8 mL of the Pt_2 complexes in water (containing 81 mg (0.070 mmol) of $K_4[Pt_2(pop)_4]\cdot 2H_2O$ and 80 mg (0.058 mmol) of $K_4[Pt_2(pop)_4I_2]$), 0.72 mL of 250 mM $H_3NC_3H_6NH_3SO_4$ aqueous solution (31 mg, 0.18 mmol), and 4.00 mL of 900 mM KNO_3 aqueous solution (364 mg, 3.6 mmol) were mixed and allowed to stand for 2 days. **2·4H$_2$O** was obtained as glossy brown cubic crystals. (144 mg, 85%).

Table 1 Mössbauer Parameters and Pt–I–Pt Distance (d(Pt–I–Pt)) for MMX Chains and Their Precursors.

	Electronic state	T / K	IS[a] / mm s^{-1}	QCC[b] / MHz	ρ_{IS}[c]	ρ_{QCC}[d]	Ref.	d(Pt–I–Pt) / Å
pop system								
1·4H$_2$O	CDW	14	0.751(15)	–1506(45)	–0.14(2)	–0.34(2)	this work	5.7623(18)[e]
1	CDW	14	0.759(15)	–1512(45)	–0.13(2)	–0.34(2)	this work	5.679[f]
2·4H$_2$O-I$_a$	ACP+CDW	14	0.639(13)	–1625(49)	–0.21(2)	–0.29(2)	this work	5.6305(8)[g]
2·4H$_2$O-I$_b$			0.359(7)	–1327(40)	–0.40(2)	–0.42(2)		5.9786(9)[g]
2	CDW	14	0.757(15)	–1471(44)	–0.14(2)	–0.36(2)	this work	5.689(2)[g]
$(H_3NC_6H_{12}NH_3)_2[Pt_2(pop)_4I]$	CDW	15	0.47(8)	–1680(50)	–0.33(5)	–0.27(2)	19b	5.916[h]
$(Et_2NH_2)_4[Pt_2(pop)_4I]$	CP	15	0.31(7)	–1567(47)	–0.43(4)	–0.32(2)	19b	6.665[i]
$K_4[Pt_2(pop)_4I_2]$	discrete	16	0.15(7)	–1530(46)	–0.54(4)	–0.33(2)	19b	
dta system								
$[Pt_2(MeCS_2)_4I]$-I$_a$	ACP	16	0.28(8)	–1180(36)	–0.45	–0.49	14d, 19a	5.914(2)[j]
$[Pt_2(MeCS_2)_4I]$-I$_b$			0.56(8)	–1380(40)	–0.27	–0.40		5.914(2)[j]
$[Pt_2(EtCS_2)_4I]$-I$_a$	ACP	11	0.35(8)	–1213(36)	–0.41(5)	–0.47(2)	19b	5.860(2)[k]
$[Pt_2(EtCS_2)_4I]$-I$_b$			0.50(8)	–1432(43)	–0.31(5)	–0.38(2)		5.917(2)[k]
$[Pt_2(MeCS_2)_4I_2]$	discrete	16	0.17(7)	–1172(35)	–0.53(4)	–0.49(2)	19b	
$[Pt_2(EtCS_2)_4I_2]$	discrete	16	0.22(7)	–1177(35)	–0.49(4)	–0.49(2)	19b	

[a] Referenced to ZnTe. [b] Converted to QCC value of ^{127}I. [c] Calculated from eq 2 in the Supporting Information. [d] Calculated from eq 4 in the Supporting Information. [e] At 100 K, see ref 17c. [f] Estimated from the lattice constant obtained from powder X-ray diffraction pattern (Lattice constant along the chain axis of **1** is 0.01 Å shorter than that of **2**.). [g] At 100 K, see ref 17b. [h] At room temperature, see ref 23. [i] At 93 K, see ref 23. [j] Calculated from the lattice constant along the chain axis and Pt–Pt distance at 91 K, see ref 24. [k] At 48 K, see ref 14f.

Dehydration Method

For dehydration, **1·4H$_2$O** was heated at 75 °C under vacuum (8×10^{-2} Pa) for 17 h, and **2·4H$_2$O** was heated at 70 °C under vacuum (8×10^{-2} Pa) for 19 h. This condition is stronger than the previous one, which can complete dehydration.[17b,c] Each dehydrated sample **1** and **2** was put into the plastic bag and sealed by the sealer in order to avoid exposure to air. The sealing was carried out in the glove bag filled with dry nitrogen gas.

^{129}I Mössbauer Spectroscopy

The 27.7 keV γ-ray generated from ^{129}Te is used for ^{129}I Mössbauer spectrum. In this study, a ^{129}Te source was obtained by the neutron irradiation of enriched ^{66}Zn^{128}Te in the nuclear reaction ^{128}Te(n,γ)^{129}Te at KUR. Since the half-life of ^{129}Te is 69.6 minutes, the measurement of ^{129}I Mössbauer spectra (typically continued for four hours) was accumulated four to six times with repeatedly-irradiated ^{129}Te source in order to obtain distinct spectra using a constant-acceleration spectrometer with a NaI(Tl) scintillation counter. The source and the absorber were cooled by a home-made closed-cycle refrigerator system using helium gas as the working medium.

Analysis of ^{129}I Mössbauer Spectra

The spectra were analyzed by the least-squares fitting with Lorentzian lines by using MossWinn software.[21] The detailed explanation of ^{129}I Mössbauer spectra are described in some references.[19,22] In the Mössbauer spectroscopy, the energy of γ-ray is controlled by changing the relative velocity of the source. The difference between the nuclear transition energy of the source and that of the absorber is called isomer shift (IS) and is customary denoted by the relative velocity to ZnTe source. The quadrupole coupling constant (QCC), which is a direct measure of the electric field gradient (EFG) at the iodine nucleus is the other important parameter available from the Mössbauer spectroscopy. The charge on the ^{129}I can be calculated from IS (ρ_{IS}) or QCC (ρ_{QCC}) as described in ESI†.

Results and Discussion

^{129}I Mössbauer Spectra of 1·4H$_2$O, 2·4H$_2$O and Their Dehydrated States

^{129}I Mössbauer spectra of **1·4H$_2$O** and **1** at 14 K are shown in Figure 2. The best fit for each spectrum was obtained with one octuplet. Therefore, there is only one chemically independent iodide site in both **1·4H$_2$O** and **1**, consistent with their CDW electronic state. As shown in Table 1, the Mössbauer parameters of **1·4H$_2$O** and **1** were nearly identical, indicating that the electronic state was not changed by the dehydration. The ^{129}I Mössbauer spectra of **2·4H$_2$O** and **2** at 14 K are shown in Figure 3. Apparently, the spectrum of **2·4H$_2$O** consists of two sets of octuplets while that of **2** consists of one octuplet. These spectra correspond to the crystal structure.[17b] Since **2·4H$_2$O** is in the ACP+CDW state, two chemically independent iodide ions exist due to the ACP-like distortion. This distortion disappears by the dehydration, therefore, the change of the ^{129}I Mössbauer spectra from **2·4H$_2$O** to **2** supports the change of the electronic state from the ACP+CDW state to the CDW state.

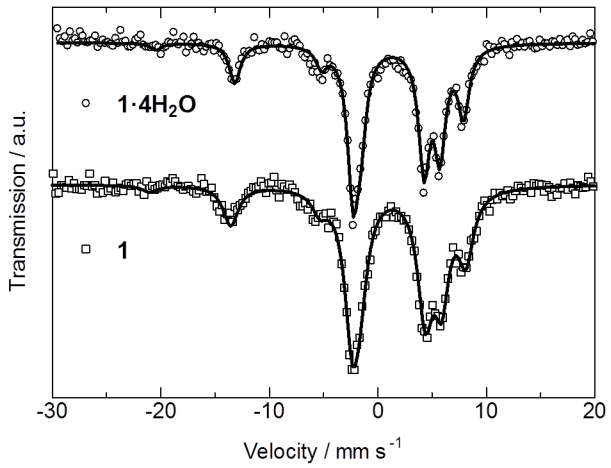

Fig. 2 ^{129}I Mössbauer spectra of **1·4H$_2$O** and **1** measured at 14 K. The solid lines were fitted with the data.

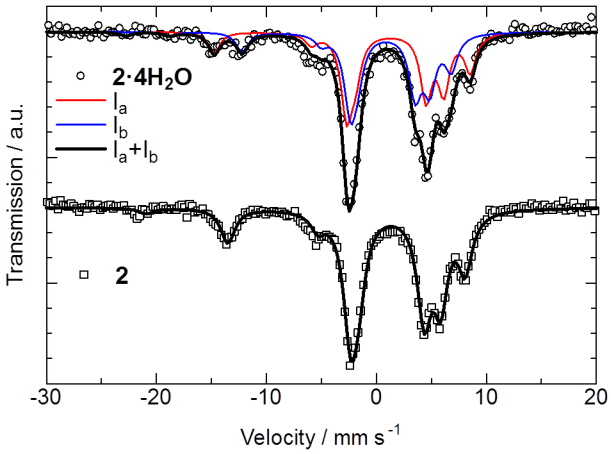

Fig. 3 ^{129}I Mössbauer spectra of **2·4H$_2$O** and **2** measured at 14 K. The red and blue solid lines indicate the I_a and I_b components, respectively. The black solid lines were fitted with the data.

Reliability of ρ_{QCC} in 1·4H$_2$O, 2·4H$_2$O and Their Dehydrated States

It has been reported that the arrangement of cations and anions around the iodide ions occasionally affects QCC value and induces inaccurate ρ_{QCC}.[19b] In **1·4H$_2$O**, **1**, **2·4H$_2$O** and **2**, the ρ_{QCC} is significantly larger than the ρ_{IS} as shown in Table 1. This difference is attributable to the characteristic molecular packing in these complexes. The three-dimensional hydrogen-bond and coordination-bond networks in present complexes constrain each [Pt$_2$(pop)$_4$] unit to arrange in the same *ab* plane, named "synchronized" packing[17c] (e.g. structure of **1·4H$_2$O** shown in Figure 4). Therefore, an iodide ion, two K^+ ion and four H$_2$O molecules (if hydrated) per formula are located in the same layer, which has positive charge in average. On the other hand, the other layer consisting of a $[Pt_2(pop)_4]^{3-}$ unit and an aliphatic diammonium ion per formula has negative charge in average. In other words, the iodide ions and the Pt ions are in the positively-charged and negatively-charged layer, respectively (Figure 4). Although the Pt ions along the *c* axis (chain axis) mainly contribute to the EFG at the iodine nucleus, the arrangement of

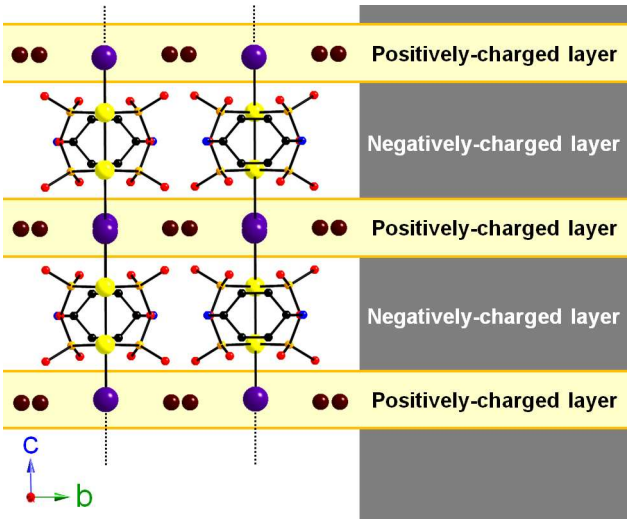

Fig. 4 Schematic representation of the charged layer in **1·4H$_2$O.** H$_2$O molecules and hydrogen atoms are omitted for clarity. Iodide ions, K^+ ions and *cis*-$H_3NCH_2CH{=}CHCH_2NH_3^{2+}$ ions are disordered. Pt yellow, I purple, K brown, P orange, O red, N blue, C black.

the charged layers should decrease the EFG, resulting in a smaller QCC and a larger ρ_{QCC} observed in the present complexes. Consequently, it can be concluded that the ρ_{QCC} is not appropriate to discuss the quantitative value of the iodine charge in the pop system. This high susceptibility of QCC to the surrounding charges are also supported by the relationship between QCC and IS as discussed in ESI† and Figure S1 therein. Therefore we focus on the ρ_{IS} from now on.

Iodine Charge of 1·4H$_2$O, 2·4H$_2$O and Their Dehydrated States

As shown in Table 1, the ρ_{IS} of **1**, **1·4H$_2$O**, and **2** are –0.13(2), –0.14(2), and –0.14(2), respectively, which are the smallest of all MMX chains. So far, the smallest values of ρ_{IS} are –0.27 for [Pt$_2$(MeCS$_2$)$_4$I] in the dta system[14d,19a] and –0.33(5) for $(H_3NC_6H_{12}NH_3)_2$[Pt$_2$(pop)$_4$I] in the pop system.[19b] Accordingly, the negative charge on the iodide ion is strongly donated to the Pt ion in the case of **1·4H$_2$O**, **1** and **2**. This result corresponds to the previous report that the covalent interaction is more dominant in the CDW state compared with the Coulomb interaction.[19b]

The two chemically independent iodide ions in **2·4H$_2$O** are denoted by I_a and I_b. The I_a locates between higher oxidized Pt ions with shorter Pt–I–Pt distance (*d*(Pt–I–Pt)), and the I_b locates between lower oxidized Pt ions with longer *d*(Pt–I–Pt). The smaller ρ_{IS} of –0.21(2) can be assigned as the value derived from the I_a in **2·4H$_2$O**, because the environment around the iodide ion in **2** (e.g. ρ_{IS} = –0.14(2), *d*(Pt–I–Pt) = 5.689(2) Å) is close to that around I_a in **2·4H$_2$O** (e.g. *d*(Pt–I_a–Pt) = 5.6305(8) Å) rather than that around I_b in **2·4H$_2$O** (e.g. *d*(Pt–I_b–Pt) = 5.9786(9) Å). Thus, the ρ_{IS} of I_b in **2·4H$_2$O** is –0.40(2). This assignment is opposite to the previous results that I_a is more negative than I_b, observed in [Pt$_2$(MeCS$_2$)$_4$I][14d,19a] and [Pt$_2$(EtCS$_2$)$_4$I],[19b] which form the ACP state. In the point-charge model, the short *d*(Pt–I–Pt) destabilize the 5d$_{z2}$ orbitals of Pt ions and stabilize the 5p$_z$ orbital of iodide ion. Therefore, the more negative iodide ion and more positive Pt ions are preferred in shorter *d*(Pt–I–Pt) if the Coulomb interaction is dominant. On the other hand, the overlap integral between these orbitals should be larger and the charge donation from

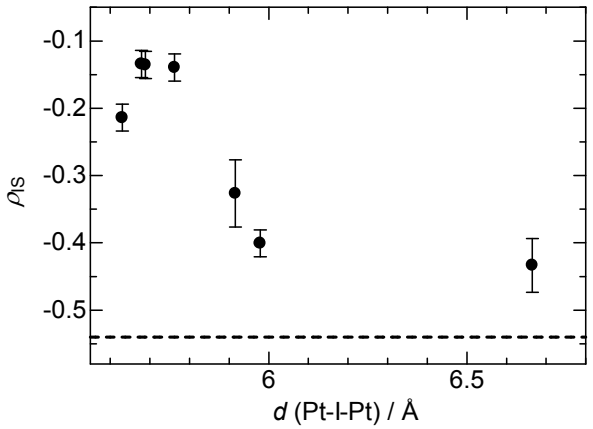

Fig. 5 Relationship between d(Pt–I–Pt) and ρ_{IS} of MMX chains in the pop system shown in Table 1. Dashed line indicates the ρ_{IS} of Pt(III)$_2$ complex, $K_4[Pt_2(pop)_4I_2]$, (ρ_{IS} = –0.54(4)).[19b] It can be regarded as the extreme value of ρ_{IS} in MMX chains (d(Pt–I–Pt) = ∞).

iodide ion to Pt ions is enhanced in shorter d(Pt–I–Pt) if the covalent interaction is dominant. Since I_a is more positive than I_b in **2·4H$_2$O**, it can be concluded that the covalent interaction predominates in the ACP+CDW state as well as the CDW state,[19b] whereas the Coulomb interaction predominates in the ACP state. This is also supported by the reported optical conductivity spectra, which reveal that the electronic structure in the ACP+CDW state is similar to that in the CDW state.[17c] Consequently, the ACP+CDW state can be regarded as the CDW state with the ACP-type lattice distortion.

The origin of the opposite result is probably the quite short d(Pt–I–Pt) in **2·4H$_2$O**. The d(Pt–I_a–Pt) in **2·4H$_2$O** (5.6305(8) Å) is 0.23 Å shorter than that in $[Pt_2(EtCS_2)_4I]$ (5.860(2) Å).[19b] In addition, the shortest Pt–I distance (d(Pt–I)) in **2·4H$_2$O** (2.641(3) Å; Figure 1) is 0.29 Å shorter than that in $[Pt_2(EtCS_2)_4I]$ (2.93 Å). Consequently, short d(Pt–I–Pt) and d(Pt–I) enhance the overlap between the orbitals and charge donation from iodide ion to Pt ions. The short d(Pt–I–Pt) in MMX chains with binary countercations originate from the coordination bonds between K^+ and oxygen atoms of pop ligands.[17c] The calculated small ρ_{IS} in the present complexes are valid even under the predominance of covalent interaction as described in ESI†.

Dependence of the Iodine Charge on Pt–I–Pt Distance

As discussed above, smaller ρ_{IS} observed in **1·4H$_2$O**, **2·4H$_2$O** and their dehydrated states indicate that the covalent interaction is stronger in MMX chains with binary countercations. It is more clearly expressed by the relationship between ρ_{IS} and d(Pt–I–Pt) as shown in Figure 5. Kobayashi et al. reported that the ρ_{IS} of discrete Pt(III)$_2$ complex in the pop system, $K_4[Pt_2(pop)_4I_2]$, is –0.54(4).[19b] This negative charge is donated to the other Pt ion at the opposite side when iodide ion bridges two $[Pt_2(pop)_4]$ units in the 1D chain. Therefore, the decrease of the d(Pt–I–Pt) increase the charge donation from iodide ion to Pt ion, resulting in smaller ρ_{IS}. The strength of the covalent interaction determines the electronic states of the MMX chains in the pop system.

On the other hand, the difference in ρ_{IS} between I_a and I_b is relatively large in the dta system, though the difference in d(Pt–I–Pt) is very small or smaller than the resolution limit of the single crystal X-ray structural analysis. Thus, there is no relationship between ρ_{IS} and d(Pt–I–Pt) in the dta system, which is consistent with the previous report that the Coulomb interaction is more dominant in the ACP state in the dta system.[19b] These difference between pop and dta system probably related to the charge of each ligand and the presence or absence of countercations. Since monovalent anionic ligand (RCS_2^-) and neutral 1D chain in the dta system produce 1D electron system without perturbation, various electronic states are observed in the same compound in the dta system (e.g. AV state above 300 K, CP state from 300 K to 80 K, and ACP state below 80 K for $[Pt_2(MeCS_2)_4I]$[14d]). This multistability is intrinsic to 1D electron system. In contrast, anionic 1D chain in the pop system require countercations, which induce the short d(Pt–I–Pt) and strong covalent interaction and thus suppress the appearance of ACP state in **1·4H$_2$O**, **2·4H$_2$O** and dehydrated complexes. Furthermore, divalent anionic ligands (pop^{2-}) and countercations can be regarded as the periodic potentials, which interfere the Coulomb interaction between Pt ions and iodide ions and thus bring about the dominance of covalent interaction. Therefore, it can be concluded that the covalent interaction plays a crucial role in the pop system and the Coulomb interaction does in the dta system.

Conclusions

The electronic states of water-vapor-responsive MMX chains in the pop system, K_2(*cis*-$H_3NCH_2CH{=}CHCH_2NH_3^{2+}$)$[Pt_2(pop)_4I]\cdot 4H_2O$ (**1·4H$_2$O**), $K_2(H_3NC_3H_6NH_3)[Pt_2(pop)_4I]\cdot 4H_2O$ (**2·4H$_2$O**) and their dehydrated complexes **1** and **2** were studied by the ^{129}I Mössbauer spectroscopy. In the case of **1·4H$_2$O**, **1** and **2**, one octuplet was observed in the ^{129}I Mössbauer spectra, consistent with the CDW electronic state. On the other hand, the spectrum of **2·4H$_2$O** consists of two sets of octuplets, corresponding to the ACP+CDW electronic state. These charges on the iodide ions (ρ_{IS}) are calculated from the isomer shift (IS) but not from the quadrupole coupling constant (QCC), which was affected by the arrangement of cations and anions. The electronic states with the exact charge of iodide ions and the formal charge of Pt ions can be represented as follows: $\cdots[Pt^{2+}\text{–}Pt^{2+}]\cdots\cdots I^{0.14-}\text{–}[Pt^{3+}\text{–}Pt^{3+}]\text{–}I^{0.14-}\cdots$ for CDW state in **2**, and $\cdots[Pt^{(2+a)+}\text{–}Pt^{(2+b)+}]\cdots I_a^{0.21-}\text{–}[Pt^{(3-c)+}\text{–}Pt^{(3-d)+}]\text{–}I_b^{0.40-}\cdots$ for ACP+CDW state in **2·4H$_2$O**. Consequently, we successfully confirmed the change of the electronic state from the ACP+CDW state to the CDW state upon dehydration by ^{129}I Mössbauer spectroscopy. The ρ_{IS} of **1·4H$_2$O**, **1** and **2** (–0.13 to –0.14) are the smallest of all MMX chains reported so far. Accordingly, the negative charge on the iodide ion is strongly donated to the Pt ion in these complexes. In **2·4H$_2$O**, more positive I_a bridges higher oxidized Pt ions with shorter Pt–I–Pt distance (d(Pt–I–Pt)) and more negative I_b bridges lower oxidized Pt ions with longer d(Pt–I–Pt). This result is opposite to the assignment in the case of the MMX chains in the dta system forming ACP state, indicating that the covalent interaction predominates in the ACP+CDW state as well as in the CDW state.[19b] Combined with the optical conductivity spectra of **2·4H$_2$O**, it can be concluded that the ACP+CDW state is regarded as the CDW state with the ACP-type lattice distortion. In the pop system, the ρ_{IS} became smaller as d(Pt–I–Pt) decreased, and thus as the charge donation from iodide ion to Pt ion

increased. In addition, pop^{2-} and countercations can interfere the Coulomb interaction between Pt ions and iodide ions. Therefore, the covalent interaction plays a crucial role in determining the electronic states of the MMX chains in the pop system.

Acknowledgments

This work was partly supported by a Grant-in-Aid for Scientific Research (S) (Grant No. 20225003) from the Ministry of Education, Culture, Sports, Science, and Technology, Japan (M. Y.), by JSPS Research Fellowships for Young Scientists (H. I.), and by the Tohoku University Institute for International Advanced Research and Education (H. I.).

Notes and references

[a] *Department of Chemistry, Graduate School of Science, Tohoku University, 6-3 Aramaki-Aza-Aoba, Aoba-ku, Sendai, 980-8578, Japan. Fax: +81-22-795-6548; Tel: +81-22-795-7643; E-mail: h-iguchi@m.tohoku.ac.jp (H. I.); yamasita@agnus.chem.tohoku.ac.jp (M.Y.)*

[b] *Core Research for Evolutional Science and Technology (CREST), Japan Science and Technology Agency (JST), 4-1-8 Kawaguchi, Saitama, 332-0012, Japan.*

[c] *Research Reactor Institute, Kyoto University, Kumatori, Sennan, Osaka, 590-0494, Japan.*

† Electronic Supplementary Information (ESI) available: Analysis of ^{129}I Mössbauer spectra and other detailed discussions including Figure S1. See DOI: 10.1039/b000000x/

1 (a) H. Akamatu, H. Inokuchi, Y. Matsunaga, *Nature*, 1954, **173**, 168–169; (b) J. P. Ferraris, D. O. Cowan, V. V. Walatka, J. H. Perlstein, *J. Am. Chem. Soc.*, 1973, **95**, 948–949.

2 H. Shirakawa, E. J. Louis, A. G. MacDiarmid, C. K. Chiang, A. J. Heeger, *J. Chem. Soc., Chem. Commun.*, 1977, 578–580.

3 C. Sauteret, J.-P. Hermann, R. Frey, F. Pradère, J. Ducuing, R. H. Baughman, R. R. Chance, *Phys. Rev. Lett.*, 1976, **36**, 956–959.

4 (a) H. Kishida, H. Matsuzaki, H. Okamoto, T. Manabe, M. Yamashita, Y. Taguchi, Y. Tokura, *Nature*, 2000, **405**, 929–932; b) S. Tao, T. Miyagoe, A. Maeda, H. Matsuzaki, H. Ohtsu, M. Hasegawa, S. Takaishi, M. Yamashita, H. Okamoto, *Adv. Mater.*, 2007, **19**, 2707–2710.

5 M. Bockrath, D. H. Cobden, J. Lu, A. G. Rinzler, R. E. Smalley, L. Balents, P. L. McEuen, *Nature*, 1999, **397**, 598–601.

6 S. Iwai, H. Okamoto, *Phys. Soc. Jpn.*, 2006, **75**, 011007–1–21.

7 H. Okamoto, M. Yamashita, *Bull. Chem. Soc. Jpn.*, 1998, **71**, 2023–2039.

8 *Material Designs and New Physical Properties in MX- and MMX-Chain Compounds*, ed. M. Yamashita and H. Okamoto, Springer-Verlag Wien, 2013.

9 M. Yamashita, D. Kawakami, S. Matsunaga, Y. Nakayama, M. Sasaki, S. Takaishi, F. Iwahori, H. Miyasaka, K. Sugiura, Y. Wada, H. Miyamae, H. Matsuzaki, H. Okamoto, H. Tanaka, K. Marumoto, S. Kuroda, *Angew. Chem. Int. Ed.*, 2004, **43**, 4763–4767.

10 K. Otsubo, Y. Wakabayashi, J. Ohara, S. Yamamoto, H. Matsuzaki, H. Okamoto, K. Nitta, T. Uruga, H. Kitagawa, *Nat. Mater.*, 2011, **10**, 291–295.

11 (a) H. Mastuzaki, H. Kishida, H. Okamoto, K. Takizawa, S. Matsunaga, S. Takaishi, H. Miyasaka, K. Sugiura, M. Yamashita, *Angew. Chem. Int. Ed.*, 2005, **44**, 3240–3243; (b) M. Yamashita, K. Takizawa, S. Matsunaga, D. Kawakami, H. Iguchi, S. Takaishi, T. Kajiwara, F. Iwahori, T. Ishii, H. Miyasaka, K.-i. Sugiura, H. Matsuzaki, H. Kishida, H. Okamoto, *Bull. Chem. Soc. Jpn.*, 2006, **79**, 1404–1406; (c) H. Iguchi, S. Takaishi, T. Kajiwara, H. Miyasaka, M. Yamashita, H. Matsuzaki, H. Okamoto, *J. Inorg. Organomet. Polym. Mater.*, 2009, **19**, 85–90.

12 (a) M. Kuwabara, K. Yonemitsu, *J. Phys. Chem. Solids*, 2001, **62**, 435–438; (b) M. Kuwabara, K. Yonemitsu, *J. Mater. Chem.*, 2001, **11**, 2163–2175.

13 (a) M. B. Robin, P. Day, *Adv. Inorg. Chem. Radiochem.*, 1968, **10**, 247–422; (b) P. Day, in *Low-dimensional cooperative phenomena*, ed. H. J. Keller, Plenum Press, New York, 1974, pp. 191–214.

14 (a) C. Bellitto, A. Flamini, L. Gastaldi, L. Scaramuzza, *Inorg. Chem.*, 1983, **22**, 444–449; (b) C. Bellitto, G. Dessy, V. Fares, *Inorg. Chem.*, 1985, **24**, 2815–2820; (c) R. J. H. Clark, J. R. Walton, *Inorg. Chim. Acta*, 1987, **129**, 163–171; (d) H. Kitagawa, N. Onodera, T. Sonoyama, M. Yamamoto, T. Fukawa, T. Mitani, M. Seto, Y. Maeda, *J. Am. Chem. Soc.*, 1999, **121**, 10068–10080; (e) M. Mitsumi, T. Murase, H. Kishida, T. Yoshinari, Y. Ozawa, K. Toriumi, T. Sonoyama, H. Kitagawa, T. Mitani, *J. Am. Chem. Soc.*, 2001, **123**, 11179–11192; (f) M. Mitsumi, K. Kitamura, A. Morinaga, Y. Ozawa, M. Kobayashi, K. Toriumi, Y. Iso, H. Kitagawa, T. Mitani, *Angew. Chem. Int. Ed.*, 2002, **41**, 2767–2771; (g) K. Otsubo, A. Kobayashi, H. Kitagawa, M. Hedo, Y. Uwatoko, H. Sagayama, Y. Wakabayashi, H. Sawa, *J. Am. Chem. Soc.*, 2006, **128**, 8140–8141; (h) M. Mitsumi, Y. Yoshida, A. Kohyama, Y. Kitagawa, Y. Ozawa, M. Kobayashi, K. Toriumi, M. Tadokoro, N. Ikeda, M. Okumura, M. Kurmoo, *Inorg. Chem.*, 2009, **48**, 6680; (i) M. Mitsumi, T. Yamashita, Y. Aiga, K. Toriumi, H. Kitagawa, T. Mitani, M. Kurmoo, *Inorg. Chem.*, 2011, **50**, 4368–4377.

15 (a) L. Welte, U. Garcia-Couceiro, O. Castillo, D. Olea, C. Polop, A. Guijarro, A. Luque, J. M. Gomez-Rodriguez, J. Gomez-Herrero, F. Zamora, *Adv. Mater.*, 2009, **21**, 2025–2028; (b) L. Welte, A. Calzolari, R. D. Felice, F. Zamora, J. Gomez-Herrero, *Nat. Nanotechnol.*, 2010, **5**, 110–115; (c) A. Guijarro, O. Castillo, L. Welte, A. Calzolari, P. J. S. Miguel, C. J. Gomez-Garcia, D. Olea, R. D. Felice, J. Gomez-Herrero, F. Zamora, *Adv. Funct. Mater.*, 2010, **20**, 1451–1457; (d) R. Mas-Balleste, J. Gomez-Herrero, F. Zamora, *Chem. Soc. Rev.*, 2010, **39**, 4220–4223; (e) C. Hermosa, J. V. Álvarez, M.-R. Azani, C. J. Gomez-Garcia, M. Fritz, J. M. Soler, J. Gomez-Herrero, C. Gomez-Navarro, F. Zamora, *Nat. Commun.*, 2013, **4**, 1709–1–6; (f) M.-R. Azani, A. P. Paz, C. Hermosa, G. Givaja, J. Gomez-Herrero, R. Mas-Ballesté, F. Zamora, A. Rubio, *Chem. Eur. J.* 2013, **19**, 15518–15529.

16 (a) C.-M. Che, F. H. Herbstein, W. P. Schaefer, R. E. Marsh, H. B. Gray, *J. Am. Chem. Soc.*, 1983, **105**, 4604–4607; (b) M. Kurmoo, R. J. H. Clark, *Inorg. Chem.*, 1985, **24**, 4420–4425; (c) R. J. H. Clark, M. Kurmoo, H. M. Dawes, M. B. Hursthouse, *Inorg. Chem.*, 1986, **25**, 409–412; (d) L. G. Butler, M. H. Zietlow, C.-M. Che, W. P. Schaefer, S. Sridhar, P. J. Grunthaner, B. I. Swanson, R. J. H. Clark, H. B. Gray, *J. Am. Chem. Soc.*, 1988, **110,** 1155–1162; (e) M. Yamashita, S. Miya, T. Kawashima, T. Manabe, T. Sonoyama, H. Kitagawa, T. Mitani, H. Okamoto, R. Ikeda, *J. Am. Chem. Soc.*, 1999, **121**, 2321–2322; (f) H. Matsuzaki, T. Matsuoka, H. Kishida, K. Takizawa, H. Miyasaka, K. Sugiura, M. Yamashita, H. Okamoto, *Phys. Rev. Lett.***,** 2003, **90**, 046401–1–4; (g) M. Yamashita, S. Takaishi, A. Kobayashi, H. Kitagawa, H. Matsuzaki, H. Okamoto, *Coord. Chem. Rev.*, 2006, **250**, 2335–2346; (h) S. Matsunaga, K. Takizawa, D. Kawakami, H. Iguchi, S. Takaishi, T. Kajiwara, H. Miyasaka, M. Yamashita, H. Matsuzaki, H. Okamoto, *Eur. J. Inorg. Chem.*, 2008, 3269–3273; (i) H. Iguchi, D. Jiang, J. Xie, S. Takaishi, M. Yamashita, *Polymers*, 2011, **3**, 1652–1661; (j) H. Iguchi, S. Takaishi, D. Jiang, J. Xie, M. Yamashita, A. Uchida, H. Kawaji, *Inorg Chem.*, 2013, **52**, 13812–13814.

17 (a) H. Iguchi, S. Takaishi, T. Kajiwara, H. Miyasaka, M. Yamashita, H. Matsuzaki and H. Okamoto, *J. Am. Chem. Soc.*, 2008, **130**, 17668–17669; (b) H. Iguchi, S. Takaishi, H. Miyasaka, M. Yamashita, H. Matsuzaki, H. Okamoto, H. Tanaka, S. Kuroda, *Angew. Chem. Int. Ed.*, 2010, **49**, 552–555; (c) H. Iguchi, S. Takaishi, B. K. Breedlove, M. Yamashita, H. Matsuzaki, H. Okamoto, *Inorg. Chem.*, 2012, **51**, 9967–6677.

18 H. Tanaka, S. Kuroda, H. Iguchi, S. Takaishi, M. Yamashita, *Phys. Rev. B*, 2012, **85**, 073104–1–5.

19 (a) H. Kitagawa, T. Sonoyama, T. Mitani, M. Seto, Y. Maeda, *Synth. Met.*, 1999, **103**, 2159–2160; (b) A. Kobayashi, S. Kitao, M. Seto, R. Ikeda, H. Kitagawa, *Inorg. Chem.*, 2009, **48**, 8044–8049.

20 C.-M. Che, L. G. Butler, H. B. Glay, *J. Am. Chem. Soc.*, 1981, **103**, 7796–7797.
21 (a) Z. Klencsár, E. Kuzmann, A. Vértes, *J. Radioanal. Nucl. Chem.*, 1996, **210**, 105–118; (b) Z. Klencsár, *Hyperfine Interact.*, 2013, **217**, 117–126.
22 (a) R. V. Parish, in *Mössbauer Spectroscopy Applied to Inorganic Chemistry*, *Vol. 2*, ed. G. J. Long, Plenum, New York, 1984, ch. 9; (b) B. Kolk, in *Dynamical Properties of Solids*, ed. G. K. Horton and A. A. Maradudin, Elsevier, New York, 1984, vol. 5, ch. 1; (c) E. Kuzmann, Z. Homonnay, S. Nagy, K. Nomura, in *Handbook of Nuclear Chemistry*, ed. A. Vértes, S. Nagy, Z. Klencsár, R. G. Lovas and F. Rösch, Springer, New York, 2nd edn., 2011, vol. 3, ch. 25.
23 K. Takizawa, Master Thesis, Tokyo Metropolitan University, 2002.
24 H. Kitagawa, S. Nakagami, T. Mitani, *Synth. Met.*, 2001, **116**, 401–404.

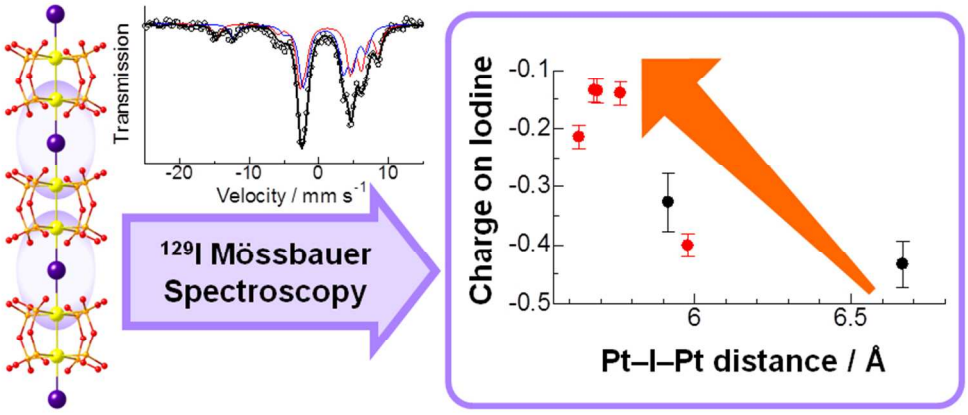

79x34mm (300 x 300 DPI)